Int J Thermophys (2008) 29:82–92
DOI 10.1007/s10765-007-0301-0

Influence of the Freezing and Annealing Conditions on the Realization of Cryogenic Triple Points

L. Wolber · B. Fellmuth

Published online: 1 November 2007

Abstract As a basis for evaluating the results of an international star comparison of sealed fixed-point cells, dedicated investigations have been directed to the dependence of the melting temperature on different conditions concerning the preparation of the solid phase, i.e., fast and slow freezing, refreezing without supercooling, or annealing at a temperature of only a few mK below the melting temperature. Differences in the typical thermophysical behavior of the four fixed-point substances hydrogen, neon, oxygen, and argon have been found. In the case of hydrogen and oxygen, the quality of the crystal lattice has little influence on the melting temperature. This enables temperature widths of the melting curves of only a few tens of μK, if there are no additional influences. On the contrary, argon samples frozen after supercooling with different velocities of freezing typically melt within a range of 0.3 mK. The melting-curve width can be reduced only by refreezing. A broader melting range of a few tenths of mK has been typically observed for neon cells. Unlike argon, an improvement of the crystal quality by a slow refreezing does not decrease the width of the melting-curve.

Keywords Cryogenic gases · Fixed points · Low temperatures · Temperature scale · Material properties

1 Introduction

The realization of the International Temperature Scale of 1990, ITS-90 [1], requires the triple points of the cryogenic gases hydrogen, neon, oxygen, and argon to be measured as defining fixed points in thermal equilibrium. This is done by measuring the melting-curve under isothermal conditions applying the intermittent heating method,

L. Wolber (✉) · B. Fellmuth
Physikalisch-Technische Bundesanstalt, Abbestrasse 2-12, 10587 Berlin, Germany
e-mail: Lutz.Wolber@PTB.de

but it should be kept in mind that the preceding freeze leaves the system in an inhomogeneous metastable state with, for instance, gradients in impurity concentrations or lattice distortions causing regions in the solid sample to yield different melting temperatures. This broadens the melting-curve and thus increases the temperature uncertainty when calibrating a thermometer. The objective of this article is to identify freezing conditions that yield flat melting-curves. Furthermore, the thermal recovery after heating is studied because it determines the dynamic temperature-measurement errors in fixed-point realizations.

The main parameter governing the formation of solid from the liquid state is the velocity of freezing, which influences the spatial distribution of impurities as well as the quality of the crystal structure. An inevitably high freezing velocity results when the cell jumps from the supercooled liquid to the first nucleation of solid, thus using the cooling energy stored in the heat capacity of the cell to instantly freeze a considerable fraction of the sample. This can be avoided only by refreezing a partially melted sample whereby the remaining solid provides a seed for crystallization. Finally, it is worth trying to remove possible lattice distortions through annealing, where the cell is kept below, but close to, its melting temperature for quite a long time.

Within the framework of an international star comparison of sealed fixed-point cells [2], a large number of quite different cells were investigated. This enabled us to look at the typical properties of the four fixed-point substances, hydrogen, neon, oxygen, and argon. In this article, the typical properties found are illustrated by describing the results obtained for selected cells as representative examples. Special emphasis is given to the properties of neon because isotopic segregation during freezing and melting seems to influence significantly both the thermal behavior during the melting-curve measurement and the temperature width of the melting-curve. After this, two shorter sections deal with oxygen and argon in comparison with neon. The properties of hydrogen are already described in detail in [3]. For this article, it is important to note that the melting curves of hydrogen samples have a very small width of only a few tens of μK in the melting region not influenced by the catalyst necessary for the spin conversion. In this case, thermal equilibrium after heating is reached very fast.

2 Measurement Method

The investigation of the sealed cells was performed by measuring the melting curves following the measurement protocol for the realization of cryogenic triple points described in [4], see also [3]. The low thermal conductivity of these fixed-point substances leads to a high internal thermal resistance R_{CS} between the metallic cell wall and the solid–liquid interface of the partly melted sample. At the highest melting fractions F, R_{CS} reaches typically some $K \cdot W^{-1}$. A heat load P on the cell will introduce a static temperature-measurement error $\Delta T = P R_{CS}$. Therefore, the melting curves are measured by intermittent heating. After each heat pulse, the cell is allowed to relax to thermal equilibrium for a sufficiently long waiting time before the final temperature reading is taken. The remaining parasitic heat load was reduced to some μW, but always kept positive. This was achieved by mounting the cell thermally isolated in the inner vacuum can of a bath cryostat, with a thermal shield held at an appropriate fixed

temperature. Such a small parasitic heat load is necessary to obtain melting curves that are not deformed by static temperature-measurement errors and makes it possible to wait several hours for thermal equilibrium without using up too much of the small heat of fusion, which may be of the order of only 10 J.

3 Results for Neon

3.1 Thermal Recovery

Compared with hydrogen [3], oxygen, and argon, the thermal recovery of neon following the heating pulses depends strongly on the freezing and annealing conditions. This is crucial to obtaining the true equilibrium melting curves and is, therefore, discussed in detail in this section.

For a cylindrical copper cell, Figs. 1 and 2 show the thermal recovery after the heat pulses to about 5% and 10% of melted sample. The dashed lines show the extrapolation of a fit to the data. The solid samples were prepared by applying four different freezing and annealing conditions: (i) fast freezing (within a few minutes) with exchange gas and supercooling, (ii) same fast freezing followed by annealing at a few tenths of mK below the melting temperature for several days, (iii) slow freezing (on the order of 10 h) in vacuum with supercooling, and (iv) slow refreezing from a melted fraction of 90%. After fast freezing, the recovery is quite fast. At $F = 5\%$, a two-hour wait is necessary to reasonably approach the final equilibrium temperature. The comparison of cases (i) and (ii) demonstrates that annealing of the solid sample does not change the recovery behavior significantly. On the other hand, the curves for cases (iii) and (iv) illustrate that, after slow freezing, a large extremely slow thermal recovery follows the first rapid fall of the temperature, requiring more than 5 h until a reading can be taken. Fortunately, in case (iii), the behavior changes at higher F values as can be seen in Fig. 3. In case (iv), the long recoveries prevail up to the highest F values, requiring measuring times that are impractical. We conclude that when measuring equilibrium neon melting curves, slow refreezing is not always a good idea. Extremely slow thermal recovery after the first heat pulses for the calorimetric realization of the triple point of neon was reported already [5], but attributed to long relaxation time constants of the isotopic spatial equilibration. A different explanation will now be given considering various sample preparations.

The dependence of the thermal recovery on the freezing and annealing conditions can be explained as follows. After fast freezing, the crystal lattice is highly distorted throughout the sample and both the impurities and the neon isotopes are homogeneously distributed. At the microscopic scale, the melting temperature is still inhomogeneous because it will be lower near crystal defects (e.g., grain boundaries—representing inner surfaces—and dislocations) and surfaces [6]. A large part of the sample portion with a lower melting temperature exists near the cell wall. Thus, the metallic body of the cell can quickly recover to the equilibrium temperature even at small values of F as shown in Figs. 1 and 2 due to the melting of these sample portions. Annealing cannot reduce the concentration of crystal defects required to change the recovery behavior.

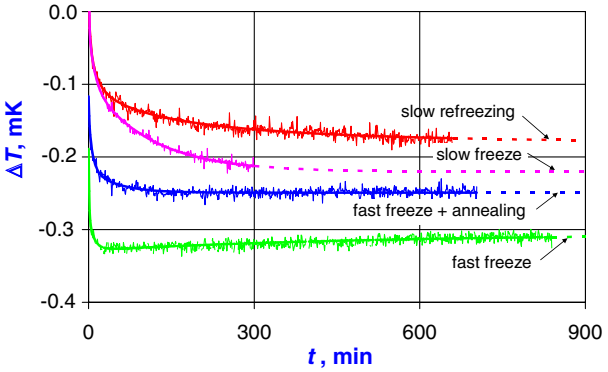

Fig. 1 (on the left) Thermal recovery at about $F = 5\%$ after freezing and annealing the neon sample under different conditions, see text. (ΔT means the deviation from the equilibrium liquidus-point temperature. Thicker lines represent fits by a superposition of exponential recovery functions)

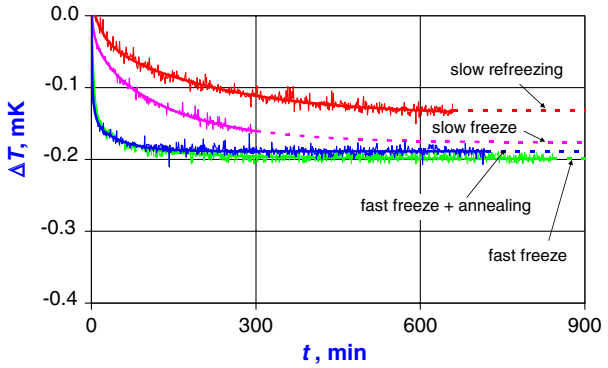

Fig. 2 (on the right) Thermal recovery at about $F = 10\%$ after freezing and annealing the neon sample under different conditions, see text

The properties of the solid neon sample after slow freezing are significantly different. The good crystal-growth condition causes much smaller concentrations of crystal defects and the melting temperature is inhomogeneous on the macroscopic scale due to the segregation of impurities and isotopes. Sample portions having the liquidus-point concentrations are solidified at the metal surfaces of the cell first. Portions with lower melting temperatures are successively frozen deeper inside the volume. When the heat pulses drive the cell above the liquidus-point temperature, sample portions adjacent to the cell wall will melt first. The first fast part of the recovery takes place until the cell reaches the liquidus-point temperature. Then, no further melting is possible near the cell wall but, especially at low F values, the system realizes that deep inside the volume there still exist regions that have an even lower melting temperature. The reaction is simultaneous refreezing of the first melted layer—providing the necessary energy—and melting of the inner regions.

This process does not violate the adiabatic condition for the cell. This reaction results in the slow recovery shown in Figs. 1 and 2 because of the low thermal

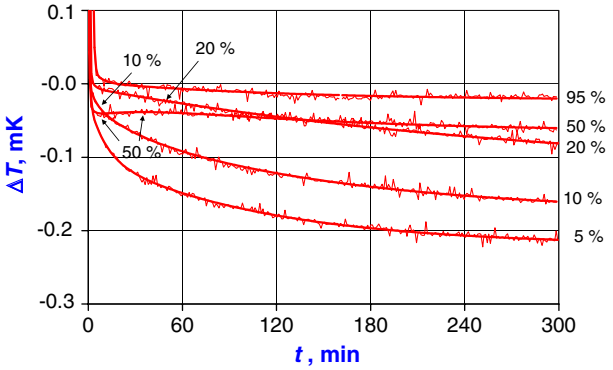

Fig. 3 Thermal recovery at different fractions of sample melted after slow freezing (about 15 h) in vacuum with supercooling (case (iii))

conductivity of solid neon. Furthermore, the refreezing may be hindered by the small temperature gradients and some surface supercooling [7]. In case (iii), only 1% of the sample freezes rapidly after the supercooling. (This explains the small influence of refreezing in case (iv) at small fractions F). In case (iii), the recovery changes at higher F values (Fig. 3), since the sample portions with stronger depressed melting temperatures are already molten, i.e., the equilibrium temperature is higher and a stable liquid layer exists near the whole cell wall. In case (iv), due to the high crystal quality at the wall, such a layer is not formed until the very end of the melting.

The slow thermal recovery after slow freezing causes a strong dependence of melting-curve results on the waiting time. This is illustrated in Fig. 4 for case (iii). Since the first fast recovery stops at the melting temperature of the sample portions adjacent to the cell wall (see above), readings taken after the fastest exponential recovery component will appear as a very flat curve close to the liquidus-point temperature, but the readings after the slowest recovery over 10 h are lower at small F values, and asymptotic values obtained by extrapolating an exponential fit to the slowest recovery yield the best information. We conclude that one should be careful when flat melting curves are claimed to result from a certain preparation. They might well be the consequence of tremendously prolonged recovery times. Such false melting curves provide no information on the inhomogeneity of the solid sample, so these curves cannot be used to support the uncertainty budget for the fixed-point realization [8].

From the above discussion, the decision whether fast or slow freezing is used to prepare the neon sample for the triple-point realization depends on the objective of the experiment. Fast freezing has the advantage that thermal recovery takes place on a manageable time scale, but during fast freezing, no segregation of impurities and isotopes occurs, thus decreasing the ability to derive information on the properties of the sample necessary to validate the cell. By melting after slow freezing, the maximum information can be obtained, but only at the expense of extremely long waiting times. This is far from practical for a realization with the aim to calibrate thermometers. A solution could be to measure the whole melting-curve using short waiting times and perform an extrapolation to the liquidus point. The curves with different slopes seem

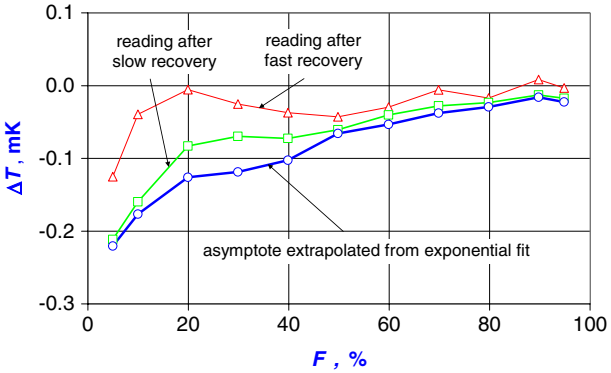

Fig. 4 Dependence of the melting-curve results after slow freezing on the waiting time. The three data sets are explained in the text

to converge at this point (see Fig. 4) due to the faster recovery at high F values. This extrapolation can be easily done with linear fits which are a good description for much of the plateau up to the highest melting fractions. But for a practical calibration at distinct F values only, a considerable uncertainty component has to be considered for the difference with respect to the asymptotic thermometer reading.

3.2 Equilibrium Melting Curves

For the four different freezing and annealing conditions discussed in the preceding section, the asymptotic melting curves were obtained by extrapolating an exponential fit to the slowest part of the recovery. These curves are the best estimate of the true equilibrium curves and are shown in Fig. 5. It is surprising that the melting-curve shape is practically independent of the freezing and annealing conditions at F values of 20% and higher. The macroscopic segregation of impurities and isotopes during the slow freezing over about 15 h may influence the recovery behavior, but it does not change the final melting-curve shape. Since the diffusion coefficients of the impurities and isotopes are very small, any contribution from segregation during freezing to the large width of the melting curves should strongly depend on the speed of freezing. The total absence of such an effect rules out a simple explanation by assuming segregation during freezing, be it due to a high impurity content, or to isotopic segregation discussed under equilibrium conditions in [9] (Moreover, the cell was filled with neon of purity 99.999%. The influence of impurities on the liquidus-point temperature is, therefore, likely not larger than (10–20) μK [10]).

Therefore, the explanation of the large temperature width of the equilibrium melting curves shown in Fig. 5 requires the melting process to be analyzed in detail. As discussed already in [11], the absence of overheating allows melting to occur also in microscopic regions throughout the whole solid sample. Near thermal equilibrium, melting starts in the sample portions having a depressed melting temperature (see above). In these microscopic regions, diffusion may be sufficient for the redistribution of isotopes. Thus, melting in the microscopic regions may take place under nearly

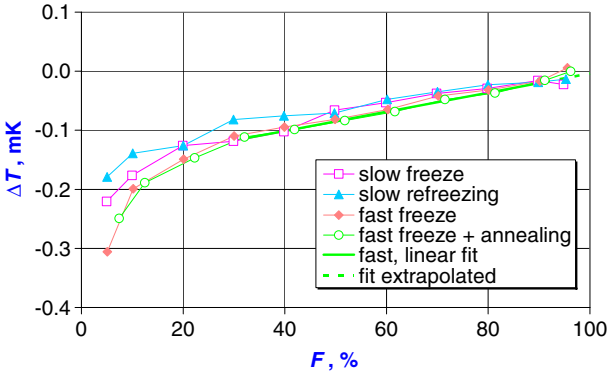

Fig. 5 Equilibrium melting curves of a neon sample contained in a cylindrical copper cell. The curves were obtained after preparing the solid sample applying quite different freezing and annealing conditions, see text

equilibrium conditions with regard to the isotope concentrations. Under these conditions, the ratio of the isotope concentrations in the adjacent microscopic solid regions and the microscopic liquid drops approaches the equilibrium distribution coefficient. The large width of the neon equilibrium melting curves is, therefore, caused by the microscopic segregation of isotopes during melting, and not by the macroscopic segregation during freezing. (By analogy, the melting in microscopic regions, a peculiarity of the melting process, broadens the melting curves of metal samples containing impurities after a fast freezing that does not allow the segregation of impurities.)

Isotopic segregation is a special problem for neon because the concentrations of the two principal isotopes are large (about 90% ^{20}Ne and 10% ^{22}Ne). Although the equilibrium distribution coefficient is suspected to be near one, the microscopic segregation may cause a significant change in the melting curve. For hydrogen, the situation seems to be different. Even for samples with the maximum deuterium content of about 155 μmol D/mol H for commercial gases, very flat melting curves of undistorted solid hydrogen have been found [3]. (The influence of the ^{22}Ne content on the neon melting temperature is about a factor of 50 smaller than that of deuterium on the melting temperature of hydrogen [3,10]). In oxygen and argon, the concentration of the dominant isotope (^{16}O and ^{40}Ar, respectively) is larger than 99.5%. For these two fixed-point substances, the influence of isotopic segregation should, therefore, be much smaller than for neon. This is supported by their very flat equilibrium melting curves, see Sect. 5. In the F range from about 40% to 90%, the equilibrium melting curves shown in Fig. 5 are highly linear. The liquidus-point temperature can be reliably determined by extrapolating a linear fit to the data in this F range.

3.3 Internal Thermal Resistance of the Cells

The dependence on F of the internal thermal resistance R_{CS} of a cylindrical copper cell filled with neon is shown in Fig. 6. For the special case (iii) of slow freezing,

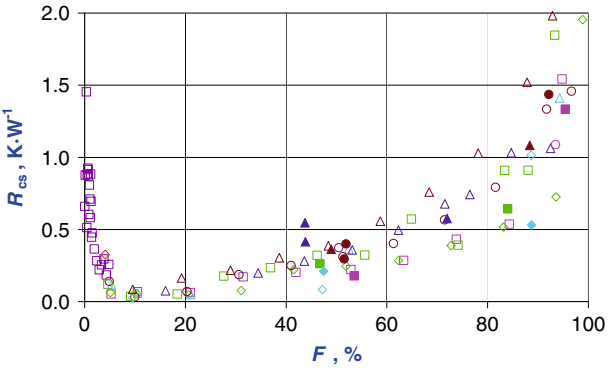

Fig. 6 The dependence on F of the internal thermal resistance R_{CS} of a cylindrical copper cell filled with neon. Data were obtained during the measurement of different melting curves

R_{CS} has been investigated in detail at F values below 5% using small heat pulses. During these heat pulses, the liquidus-point temperature was not reached, i.e., melting could not take place in the sample portions adjacent to the cell wall, but only deep inside the volume. Under these conditions, R_{CS} is a mean thermal resistance of the solid between the cell wall and the sample portions having a sufficiently low melting temperature. The low thermal conductivity of the solid causes relatively large mean R_{CS} values. At F values above 5%, the temperature during the heat pulses was higher than the liquidus-point temperature and layers close to the inner metal surface of the cell were melted. In this situation, R_{CS} reflects only the thermal resistance across the liquid layer between the cell wall and the nearest solid. The increase of R_{CS} at higher F values is caused by the larger thickness of the liquid layer. Maximum R_{CS} values of about $2\,\mathrm{K{\cdot}W^{-1}}$ require a reduction of the parasitic heat load below $10\,\mu\mathrm{W}$ if the static temperature-measurement errors are to be kept smaller than $20\,\mu\mathrm{K}$. The absence of any increase in slope at the end of the equilibrium melting curves presented in Fig. 5 verifies that this has been achieved during the measurements.

4 Results for Oxygen and Argon

4.1 Oxygen

Except near their beginning, the equilibrium melting curves of oxygen samples are very flat with temperature widths of only a few tens of μK. This was demonstrated for sealed triple-point cells of quite different design in [2]. In Fig. 7, it is shown that the shape of the melting curves obtained for a cylindrical copper cell filled with oxygen is influenced by the conditions used for the preparation of the solid sample only up to 5% of sample melted. This is surprising in view of the fact that about 15% of the sample froze rapidly after the supercooling. (Oxygen has the largest supercooling of the four cryogenic gases under consideration, ranging up to about 1.5 K). Thus, the melting temperature of oxygen seems to be extremely insensitive to distortions of the crystal lattice.

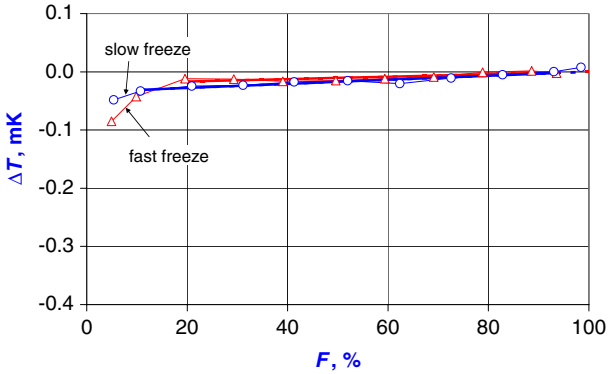

Fig. 7 Equilibrium melting curves obtained for a cylindrical copper cell filled with oxygen after slow (1,200 min) and fast freezing (5 min). (For comparison purposes, the vertical axis has a range which is similar to that of the other figures showing melting curves)

This situation is similar to that for hydrogen, if the melting temperature is not influenced by the spin-conversion catalyst [3]. The flat melting curves and the small spread (less than 0.1 mK) of the triple-point temperatures of many oxygen cells reported in [2] demonstrate, furthermore, a sufficiently small influence of impurities in commercial oxygen samples. For the curves given in Fig. 7, the liquidus temperature can be reliably determined by extrapolating a linear fit to the melting-curve data, yielding a nearly horizontal line at the 20 μK level in the F range from about 20% to 90%. In view of the discussion of the recovery behavior of neon cells in Sect. 3.1, the favorable properties of oxygen samples have another consequence: the recovery is fast due to the absence of large gradients of the melting temperature inside the solid sample. The necessary waiting times after the heat pulses amount to, at most, 2 h at the few 10 μK level for appropriately designed cells, even at low F values. At high F values, thermal equilibrium can be reached after 10 min (order of magnitude), which is a significant advantage compared with neon samples.

4.2 Argon

The three equilibrium melting curves in Fig. 8 demonstrate that, compared with hydrogen, oxygen, and neon, the melting temperature of argon is very sensitive to distortions of the crystal lattice. The curves were obtained for a cylindrical stainless-steel cell after different preparations of the solid sample: fast (about 9 min) and slow freezing (about 22 h) after supercooling, as well as slow refreezing (about 20 h) from a 90% melted fraction. After the supercooling, about 4% of the sample froze very rapidly. Nevertheless, the melting temperature is depressed by crystal defects up to about $F = 40\%$ after fast freezing. This can be understood as the consequence of starting further crystal growth from the poor structure produced by the rapid freezing during the jump from the supercooled state to the melting temperature. The situation persists for low freezing velocities, with only slight improvement. The decisive improvement comes with refreezing. The refreezing enables good crystals to be grown from the very beginning

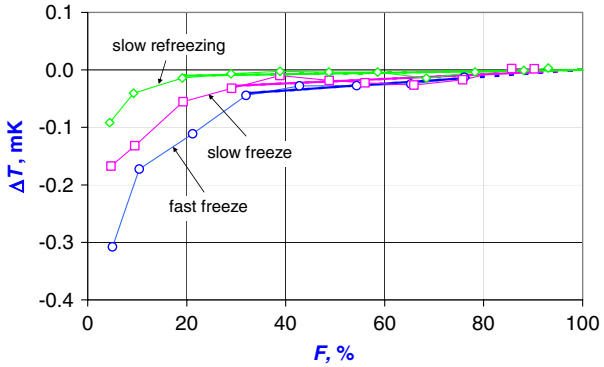

Fig. 8 Equilibrium melting curves obtained for a cylindrical stainless-steel cell filled with argon after different preparations of the solid sample: fast and slow freezing after supercooling as well as slow refreezing from $F = 90\%$

because at $F = 90\%$ the remaining solid sample portions, which act as seeds, have high crystal quality, and supercooling is avoided. A decrease of the temperature width of the argon melting curves was reported in [12], and also mentioned in [2,13], but the tentative explanation given in [13] does not consider the influence of crystal defects.

After refreezing, the dependence of the equilibrium melting temperature on F shown in Fig. 8 is very flat in the range from 20% to 90% (temperature width of only about 10 μK) and highly linear. This allows the liquidus-point temperature to be determined with a small uncertainty of the order of 10 μK.

Due to the very low microscopic and macroscopic inhomogeneity of the melting temperature, which is verified by the flat melting curves, the thermal recovery is fast (necessary waiting time about 1 h) for all F values from 5% to 95%, after refreezing. A slower recovery (waiting time about 2 h) has been observed after fast freezing only up to about $F = 10\%$. This is comparable to the recovery of neon after fast freezing (see Sect. 3.1) and is caused by the existence of microscopic inhomogeneity of the melting temperature due to the high concentration of crystal defects.

5 Conclusions

Dedicated investigations of the thermophysical properties of the three fixed-point substances neon, oxygen, and argon were performed by determining the parameters of sealed cells filled with these cryogenic gases. (The results of similar investigations of hydrogen are described in [3]). These experiments were especially directed to the dependence of the melting-curve on the following methods to prepare the solid phase for the triple-point realization: fast and slow freezing, re-freezing without supercooling, and annealing at a temperature of only a few mK below the melting temperature.

Differences in the typical properties of hydrogen, neon, oxygen, and argon have been found. In the case of hydrogen and oxygen, the quality of the crystal lattice has little influence on the melting temperature. This enables temperature widths of the melting curves of only a few tens of μK if there are no additional influences, e.g.,

the extreme distortion of the crystal lattice by the spin-conversion catalyst used in hydrogen cells. On the contrary, argon samples frozen after the supercooling with different velocities of freezing typically melt within a range of about 0.3 mK. The melting-curve width can only be reduced by a refreezing without supercooling, starting from a sample containing some solid phase on which the solid can grow. A broader melting range of a few tenths of mK has been typically observed for neon cells but, unlike argon, an improvement of the crystal quality by a slow refreezing without supercooling does not decrease the width of the melting curve. The broad melting range seems to be caused by isotopic segregation in microscopic regions during melting.

For the fixed-point realization applying the intermittent-heating technique, the thermal recovery after heating is of practical importance because it determines the dynamic temperature-measurement errors. Here, neon also has particular properties compared with the three other fixed-point substances. Although the macroscopic segregation inhomogeneities of the isotope concentrations after slow freezing are small, they cause extreme long recovery times. Depending on the objective of the fixed-point realization, one must decide which freezing conditions and waiting times between the end of heating and temperature measurement should be used.

References

1. H. Preston-Thomas, Metrologia. **27**, 3 (1990)
2. B. Fellmuth, D. Berger, L. Wolber, M. de Groot, D. Head, Y. Hermier, Y.Z. Mao, T. Nakano, F. Pavese, V. Shkraba, A.G. Steele, P.P.M. Steur, A. Szmyrka-Grzebyk, W.L. Tew, L. Wang, D.R. White, in *Temperature: Its Measurement and Control in Science and Industry*, Part 2, ed. by D.C. Ripple (AIP, New York, 2003), pp. 885–890
3. B. Fellmuth, L. Wolber, Y. Hermier, F. Pavese, P.P.M. Steur, I. Peroni, A. Szmyrka-Grzebyk, L. Lipinski, W.L. Tew, T. Nakano, H. Sakurai, O. Tamura, D. Head, K.D. Hill, A.G. Steele, Metrologia **42**, 171 (2005)
4. B. Fellmuth, D. Berger, L. Wolber, in *Proceedings of TEMPMEKO '99, 7th International Symposium on Temperature and Thermal Measurements in Industry and Science*, ed. by J.F. Dubbeldam, M.J. de Groot (Edauw Johannissen bv, Delft, 1999), pp. 233–238
5. H. Sakurai, Trans. Soc. Instr. Control Eng. **35**, 144 (1999) [in Japanese]
6. P. Papon, J. Leblond, P.H.E. Meijer, *The Physics of Phase Transitions* (Springer Verlag, Berlin, Heidelberg, New York, 2002)
7. W. Kleber, *Einführung in die Kristallographie* (VEB Verlag Technik, Berlin, 1982), p. 190
8. B. Fellmuth, K.D. Hill, P. Bloembergen, M. de Groot, Y. Hermier, M. Matveyev, A. Pokhodun, D. Ripple, P.P.M. Steur, *Working Documents of the 23rd Meeting of the Consultative Committee for Thermometry*, BIPM, document CCT/05-08 (2005)
9. J.L. Tiggelman, *Low-temperature Platinum Thermometry and Vapour Pressures of Neon and Oxygen* (Thesis, KOL, Leiden, 1973)
10. F. Pavese, B. Fellmuth, K.D. Hill, D. Head, Y. Hermier, L. Lipinski, T. Nakano, A. Peruzzi, H. Sakurai, A. Szmyrka-Grzebyk, A.D. Steele, P.P.M. Steur, O. Tamura, W. L. Tew, S. Valkier, L. Wolber, Progress Towards the Relationship Temperature vs. Isotopic Composition of Neon, in *Proceedings TEMPMEKO 2007* (submitted to *Int. J. Thermophys.*)
11. B. Fellmuth, K.D. Hill, Metrologia. **43**, 71 (2006)
12. H. Sakurai, in *Proceedings of TEMPMEKO '99, 7th International Symposium on Temperature and Thermal Measurements in Industry and Science*, ed. by J.F. Dubbeldam, M.J. de Groot (Edauw Johannissen bv, Delft, 1999), pp. 124–128
13. T. Nakano, O. Tamura, H. Sakurai, in *Proceedings of TEMPMEKO 2004, 9th International Symposium on Temperature and Thermal Measurements in Industry and Science*, ed. by D. Zvizdić, L.G. Bermanec, T. Veliki, T. Stašić (FSB/LPM, Zagreb, Croatia, 2005), pp. 159–164